Phys. Chem. Glasses: Eur. J. Glass Sci. Technol. B, August 2007, **48** (4), 201–217

Diffusion processes in vitreous silica revisited

Marcio Luis Ferreira Nascimento & Edgar Dutra Zanotto

Vitreous Materials Laboratory, Department of Materials Engineering, Federal University of São Carlos 13595-905, São Carlos-SP, Brazil

We analysed literature data on crystal growth rate, u, viscosity, η, and diffusivities of silicon and oxygen, between the glass transition, T_g, and the melting point, T_m, for four types of commercial silica glasses and thin films. The self-diffusion coefficients and the viscosity in this network glass are extremely dependent on the impurity level, much more than in multi-component, depolymerised, silicate glasses. Despite this drawback, we have combined such kinetics data in a systematic way and confirmed that normal growth is the operative mechanism of crystal growth. The effective diffusivity for viscous flow, D_η, and the controlling activation energy were compared with the activation energies and diffusivities calculated from crystal growth rates, D_u, and with those for silicon and oxygen diffusion rates (D_{Si} and D_O, respectively). In the whole temperature range $D_u \approx D_\eta \approx D_{Si}$, but oxygen diffusivities are much higher than $D_u \approx D_\eta \approx D_{Si}$. We speculate that this fact can be explained because non-bridging oxygens diffuse much faster than bridging oxygens (more easily measured experimentally); or perhaps Si and bridging oxygen do not diffuse together. There is no sign of decoupling between silicon diffusivity and viscous flow from the melting point down to T_g. We thus conclude that silicon controls the transport mechanism involved in crystal growth and viscous flow in this glass.

1. Introduction

Crystal growth kinetics in glass forming liquids have been extensively studied.[1–11] In stoichiometric systems which undergo glass to crystal transformation without compositional changes, crystal growth should be controlled by reactions at the crystal/melt interface and is normally described by one of three classical phenomenological models: normal (or continuous) growth, screw dislocation growth, and 2D surface nucleated growth. However, for only a few stoichiometric glass forming oxide systems crystal growth rates have been measured in wide temperature ranges, from approximately T_g to T_m (e.g. SiO_2, GeO_2, $Na_2O.2SiO_2$, $Li_2O.2SiO_2$, $K_2O.4B_2O_3$, diopside, cordierite and perhaps a few others). These few glasses have been the subject of numerous investigations. Nevertheless, the crystal growth mechanism is thought to be known for only a few: e.g. GeO_2, SiO_2 – normal growth;[6,12] $Na_2O{\cdot}2SiO_2$ and diopside – screw dislocation;[7,11] and $K_2O.4B_2O_3$ – 2D nucleated growth.[8] In addition, diffusion data for the slowest moving species in such glasses – Si, B, Ge, and O – are scarce and thus the precise mechanism of diffusive transport controlling crystal growth in such glasses and in most of the non-stoichiometric systems remains unknown.

Silica (SiO_2) is an important mineral from a geological standpoint and is also the most important glass former. In addition, high silica glasses having >99·9% SiO_2, best known as quartz glass, fused quartz or vitreous silica, have a plethora of important commercial applications, such as laboratory glassware, telescopic mirrors, optical filters and fibres.

In the existing literature one can find kinetic data: e.g. crystal growth rates,[12–33] viscosities[34–77] and self diffusion coefficients for several silica glass types having distinct impurity levels, as described below. However, most of these previous studies do not cover wide temperature ranges, and comparisons between different silica glass types can be rather difficult and confusing. But we will show below that such difficulties can be overcome. Furthermore, as thermodynamic and kinetic data, such as melting enthalpy and viscosity are available for silica, quantitative comparisons between crystal growth models and experiments are facilitated.

Silica glass manufacturers generally divide the whole spectrum of commercial transparent silica glasses into several types, depending on the starting materials, production method, content and type of impurities, such as alkali and metal ions, OH^- and chlorine:[78]

Type I – glasses obtained by melting natural or synthetic quartz in electrical furnaces. Such glasses contain about 30 ppm alkali and metal impurities such as Li, Na, K, Al, Fe, Ti, Ca, etc., inherited from the initial raw material, but less than 30 ppm 'water'. Examples of commercial products are: Infrasil, GE 124, 125, 201 and 204a, KI, KS4V, Puropsil A and B, Pursil, Rotosil, T-2030 and IR Vitreosil.

[1] Corresponding author. Email pmlfn@iris.ufscar.br & dedz@power.ufscar.br

Proceedings of the Eighth International Otto Schott Colloquium, held in Jena, Germany on 23–27 July 2006.

Type II – glasses obtained by melting natural or synthetic quartz in hydrogen–oxygen or natural gas flames. Glasses of this type contain about 30 ppm impurities inherited from the starting quartz grains and several hundred ppm of structural water. Examples of commercial products are: Ilmasil, Armesil T-08, Heralux, Herasil, Herasil I, Homosil, KU-2, KV, OG Vitreosil, Optosil I, II and III, Ovisil 451, T-1030, T-08 and Ultrasil.

Type III – glasses obtained by high temperature hydrolysis of volatile compounds of silicon. Such glasses are characterised by very low content of metal impurities (<1 ppm), but contain a considerable concentration of structural water (1000 ppm) and ~100 ppm chlorine. Examples of commercial products are: Corning 7940, Dynasil 4000, KU-1, GE151, Spectrosil H and V, Suprasil I and II, Synsil and T-4040.

Type IV – glasses obtained by high temperature oxidation of $SiCl_4$. Glasses of this type contain very small amount of metal impurities (less than 0·1 ppm) and only 1 ppm structural water. However, they contain several hundred ppm of chlorine. Examples of commercial products are: Corning 7943, KUVI, Spectrosil WF, Suprasil W, W1 and W2.

Also, a new synthetic silica glass was produced by sintering a sol-gel derived powder into a glass. Contamination levels of about 0·1 ppm OH^- and 400 ppm Cl^- are typical for this type of silica. Unfortunately the nature of the sintering process makes it inappropriate for optical uses, and especially for large samples production. This silica variety and others will not be considered in this work due to scarcity of available data. To the best of our knowledge, thin film silica glasses have not yet been clearly categorised. Table 1 shows some examples of the typical impurity contents in the first four types of silica glasses.

Several studies have been carried out about the crystallisation kinetics of different types of silica glasses. However, crystallisation and melting of cristobalite in a wide range of undercoolings, which included the region of maximum growth rate, were performed long ago by Wagstaff.[12–13] As far as we know, there is no new crystal growth data for any silica type in such wide range of temperatures. We will thus extensively use Wagstaff's data in this article.

2. Objectives

Despite the difficulties with its extreme sensitivity to impurities, silica glass is, in principle, a good model system for the type of study proposed here for a number of reasons: it undergoes polymorphic crystallisation, there is plenty of viscosity and crystal growth rate data available, as well as thermodynamic properties – such as melting point and Gibbs free energy of crystallisation (ΔG) – which substantially helps the analysis. An important additional motivating factor is that (hard to measure) self diffusion coefficients of oxygen (D_O) and particularly of silicon (D_{Si}), the slowest diffusing species in silicate glasses, are also available for some silica types.

In the present work we collected and combine crystal growth rates, viscosity and diffusion data for each distinct silica glass type over a broad temperature range. We then estimate the temperature rise in the crystal/melt interface to correct the crystal growth rates, and assess the applicability of the classical phenomenological theories of crystal growth. As these kinetic properties are extremely dependent on the impurity level, much more than in multicomponent, depolymerised, silicate glasses, to overcome the problem of analysing data from different authors we compare crystal growth, viscosity and self diffusion data for analogous silica glass types, having similar impurity contents. We use the same strategy proposed and tested in Nascimento *et al*[10] for diopside to infer which ion(s) control the crystal growth kinetics and viscous flow in undercooled liquid silica. We first check the crystal growth mechanism and then compare the effective diffusion coefficients determined in three distinctive ways, i.e., calculated from crystal growth rates, D_u, estimated through viscosity data, D_η (via the Eyring relation), and directly measured

Table 1. Common silica impurity contents used in this paper (approximated values)

Type	*Brand name*	*Tracer elements (ppm)*	*OH^- (ppm)*	*Cl^- (ppm)*
I	Puropsil A / B	Al (25), Ca (1·0), Fe (0·5), Li (1·0), Na (0·5), Ti (0·8), K (0·5) Total ≈29	≈8	-
I	GE 124	Al (20·3), Ca (1·8), Fe (1·9), Li (1·0), Mg (0·5), Mn (0·1), Na (1·3), Ti (1·4), Zr (2·4) Total ≈31	33	-
I	Heraeus Quarzglas / Infrasil	Al (20), Ca (1·0), Fe (0·8), Li (1·0), Mg (0·1), Na (1·0), Ti (1·0), Cr (0·1), Cu (0·1), K (0·8) Total ≈26	≈10	-
II	Vitreosil	Al (15), Ca (0·5), Fe (0·1), Li (0·2), Zr (1·3), Na (0·1), Ti (1·3), K (0·2) Total ≈18·7	170	-
III	Spectrosil	Al (0·02), Ca (0·01), Fe (0·01), Li (0·01), Mg (0·01), Na (0·01), Ti (0·01), Cr (0·01), Cu (0·01), K (0·01) Total ≈0·16	1000	100
IV	Suprasil W	Al (0·01), Ca (0·015), Fe (0·005), Li (0·001), Mg (0·005), Na (0·01), Ti (0·005), Cr (0·001), Cu (0·003), K (0·01) Total ≈0·065	1	200

self diffusion coefficients of silicon and oxygen, for each silica glass type. Our aim is to assess which ions or 'molecular units' control viscous flow and crystallisation rates. Another point we wanted to verify is if the (often used) viscosity coefficient is capable of describing molecular transport at the crystal/liquid interface during crystal growth.

We thus analyse the transport mechanism that controls crystal growth kinetics and viscous flow in undercooled liquid silica in detail, in a wide temperature range, using independent, reliable experimental data on the thermodynamic driving force, viscosity, diffusion coefficients and crystal growth rates. As the diffusion mechanisms involved in crystal nucleation and growth are unknown for most glasses, we go deeper into this question, by relating crystal growth kinetics with both viscous flow and directly measured diffusion data. Following a previous work that focused only in the diffusion process on type I silica,[79] this paper addresses the subsequent question: do crystal growth rates, diffusivities and viscous flow have different behaviours in the various silica glass types? Finally, we test the influence of impurities on the oxygen and silicon self diffusion in bulk and thin film silica glasses.

3. Theory

Three phenomenological models are frequently used to describe crystal growth kinetics controlled by atomic or molecular rearrangements at the crystal-liquid interface: normal growth, screw dislocation growth and growth controlled by 2D surface nucleation.[1] According to Jackson's treatment of the interface,[80] materials with small entropy of fusion, such as silica (ΔS_m=0·46R, R is the gas constant, in J/mol K), are expected to exhibit crystal growth kinetics of the form predicted by the normal growth model.

According to the normal model, the interface is rough on an atomic or molecular scale. Growth takes place at step sites intersecting the interface, and the growth rate, u, may be expressed by

$$u = f\frac{D_u}{\lambda}\left[1-\exp\left(-\frac{|\Delta G|}{RT}\right)\right] \quad (1)$$

where D_u is an effective diffusion coefficient (m^2/s) of the (unknown) species that controls atomic or molecular attachment at the interface; λ is the (unknown) diameter of the diffusing building molecules (m), which is equivalent to the jump distance, the lattice parameter or the unit distance advanced by the interface; ΔG is the free energy change upon crystallisation (J/mol); T is the absolute temperature (K), and f is the fraction of preferred growth sites on the interface, that is close to unity.

To interpret experimental data with respect to the kinetic models described above, it is necessary to evaluate the diffusivity D_u. This parameter can be estimated with the Eyring (or Stokes–Einstein) equation, assuming that the molecular motions required for interfacial rearrangements controlling crystal growth is similar to those controlling viscous flow in the bulk liquid, $D_u \cong D_\eta$. Hence

$$D_\eta = \frac{k_B T}{\lambda\eta} \quad (2)$$

where η is the shear viscosity (Pa s) and k_B is the Boltzmann constant. The Eyring (E) and Stokes–Einstein (SE) equations differ only by a factor of 3π. The SE expression describes a moving solid sphere with radius r in a viscous liquid. Thus, for silicate glasses most authors prefer the Eyring equation because the physical meaning of λ, the jump distance, is most appropriate (Equation (2)). Nevertheless, the overall conclusions of this paper would not be altered if we employed the SE equation.

It has been a matter of strong discussion if the Eyring equation can be used for calculations of crystal growth kinetics, especially at deep undercoolings, below 1·2T_g, where it has been suggested that this equation fails (e.g. see Ref. 10 and references cited therein). In this paper the Eyring equation (Equation (2)) is supposed to be valid from near melting to temperatures well below ≈1·2T_g, covering thus a wide temperature range.

It is clear from the above discussion that one needs to know the glass viscosity as a function of temperature and other experimental parameters, such as ΔH_m (or ΔG) and T_m, to compute crystal growth rates to compare theoretical predictions with experimental results. The melting enthalpy, ΔH_m, of silica is approximately 7680 J/mol.[12–13] The energy barrier, ΔG, can be estimated in two ways: by the Thomson/Turnbull (Equation (3a) or Hoffman (Equation (3b)) approximations. These give an upper and lower bound to ΔG, respectively

$$\Delta G = \frac{H_m(T_m - T)}{T_m} \quad \text{(Thomson)} \quad (3a)$$

$$\Delta G = \frac{H_m(T_m - T)T}{T_m^2} \quad \text{(Hoffman)} \quad (3b)$$

As previous results[10] of a kinetic analysis obtained by these two approximations (Equations (3a–b)) are almost identical in a wide temperature range here we use only Thomson's (Equation (3a)).

4. Results

4.1. Available crystal growth rates in the literature

Figures 1–4 show that the crystal growth rates in silica glasses[12–33] are strongly influenced by the

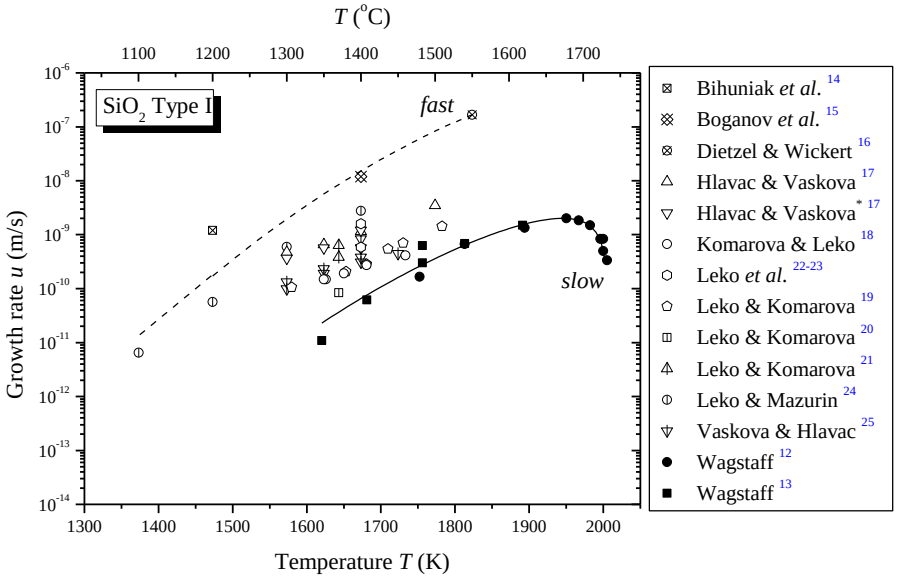

Figure 1. Crystal growth rates of type I silica glasses. The lines are fitted curves using the normal growth equation with λ=0·16 and 2 Å, corresponding to two crystal growth regimes: fastest (dashed line) and slowest (full line), using the lowest and highest viscosity data for each case, respectively – see discussion

impurity content, i.e. glasses from different sources show widely distinct growth kinetics. Fortunately the exact types of silica glasses used here were reported except for three particular cases. For the other glasses we inferred the types from the fabrication procedure, total impurity content, water level, or commercial brand name, according to Sciglass 5.0.(78)

Figure 1 shows two limiting sets of crystal growth rates and an intermediate one for type I silicas. Wagstaff's data,(12,13) which also includes the maximum u_{max}, span over two orders of magnitude and show the slowest u among all type I glasses. He used a glass with the following impurities in ppm: Al_2O_3 (137), Fe_2O_3 (5), TiO_2 (3), CaO (8), MgO (4), K_2O (2), Na_2O (27) and Li_2O (0·7). The OH^- content in type I glass is typically below 30 ppm, as demonstrated in Table 1. Wagstaff observed some crystals growing in the glass interior. His samples were prepared by cutting cubes from a piece that had been treated for 70 h at 1773 K to develop internal crystallisation centres (which were probably catalysed on solid heterogeneities). The kinetics of crystal growth and melting were determined by measuring the incremental dimensional change of any selected crystal occurring after further heat treatment. This technique required the removal of surface devitrification and polishing of two opposite

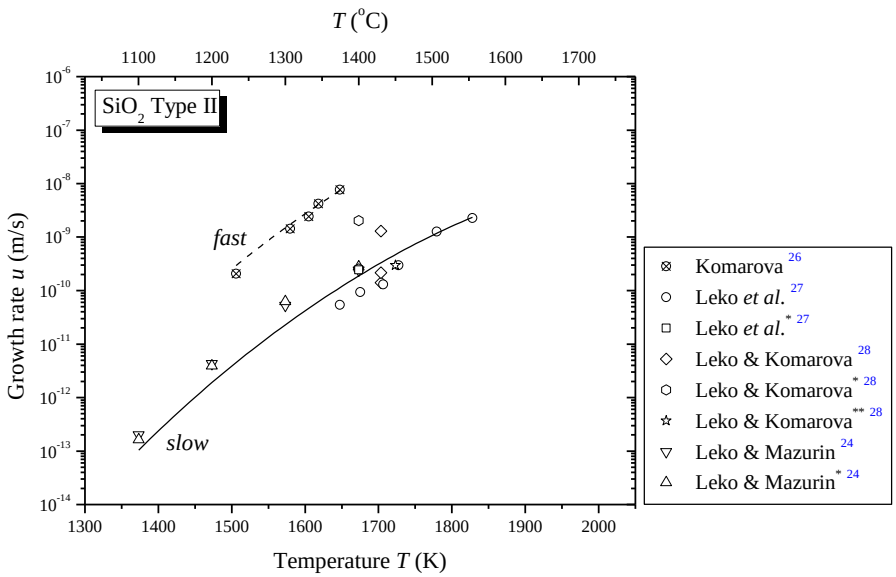

Figure 2. Crystal growth rates of type II silica glasses. The lines are fitted curves using the normal growth model, with λ=0·26 and 0·15 Å corresponding to the fastest (dashed line) and slowest (full line) crystal growth rates, using the lowest and highest viscosity data for each case, respectively – see discussion

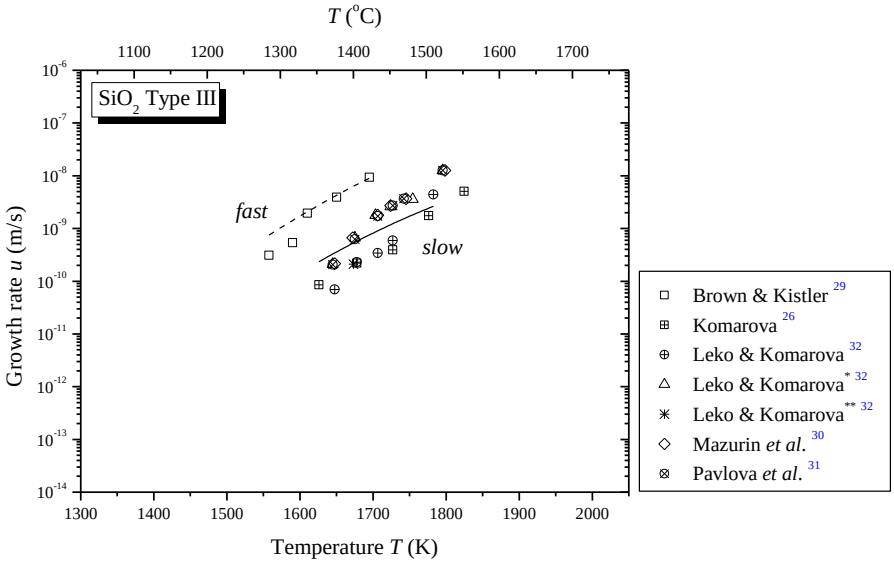

Figure 3. Crystal growth rates of type III silica glasses. The lines are fitted curves using the normal growth model, with λ=0·3 and 1 Å, corresponding to fastest (dashed), and slowest (full line) crystal growth regimes. In this case we used the general viscosity curve corresponding to this glass type – see discussion

faces before microscopic measurements.

Figure 2 refers to type II silica and shows two different data sets. Figure 3 also shows two data sets for type III glass, the same as Figure 4 for type IV glass.

For type I glasses we used data from the following sources: Bihuniak *et al*[14] measured the thickness of crystallized layers using an optical microscope at 1623 K. Boganov *et al*[15] used the same technique at 1673 K, while Dietzel & Wickert[16] measured *u* at 1823 K. Hlavac & Vaskova[17] measured the crystalline layer in two type I quartz glasses denominated Czechoslovakian and French [*] between 1573–1773 K. Komarova & Leko[18] used a KI type I glass. Leko & Komarova[19] also used KI glass, and two other type I silica glasses.[20–21] Leko *et al*[22–23] used an unknown type I silica glass. Judging from the water content, Leko & Mazurin[24] probably used a type I silica glass. Vaskova & Hlavac[25] measured the growth of the crystal layer between 1573–1673 K. Wagstaff[12–13] used a type I SiO_2 glass.

Regarding type II SiO_2 glass, Komarova[26] melted some glasses and studied the crystal growth rates on the sample surfaces. Leko *et al*[27] measured the crystallized thickness in a KU-2 tube and block glass [*]. Leko & Komarova[28] also used a KU-2 type

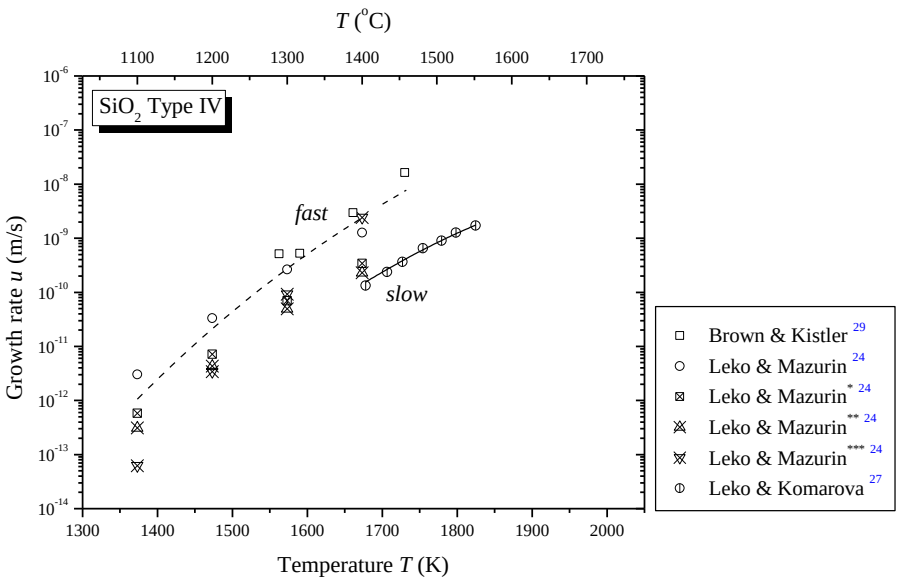

Figure 4. Crystal growth rates of type IV silica glass. The lines are fitted curves using the normal growth model, with λ=0·77 and 0·8 Å, corresponding to fastest (dashed) and slowest (full line) crystal growth rates using the lowest and highest viscosity data for each case, respectively – see discussion

II glass at 1673 K and 1723 K [*], and a third type II glass between 1373–1673 K [**]. Leko & Mazurin[24] measured u between 1273–1673 K using two different type II [*] silica glasses.

Regarding type III SiO_2 glass, Brown & Kistler,[29] Mazurin *et al*[30] and Pavlova[31] used Corning 7940 glass. Komarova[26] synthesed hers in vapor phase in a hydrogen–oxygen flame using $SiCl_4$. Leko & Komarova[32] also used two KU-1 [*] and a Corning 7940 glass [**].

Finally, regarding type IV SiO_2 glass, Leko *et al*[27] used a KUVI glass made by synthesis in vapor phase, in oxygen-containing $SiCl_4$ plasma. Leko & Mazurin[24] measured the crystal layer between 1273–1673 K [*, **, ***] in four (estimated) type IV silica glasses. Brown & Kistler[29] used a Cab-O-Sil-'0' glass and studied the growth rate of the crystal layer on the glass surface. We are not aware of crystal growth measurements in Type V and in silica glass films.

4.2. Viscosity data from the literature

As regards to viscosity data, we followed the same procedure used to analyse crystal growth rates. For type I glasses we considered data from the following authors: Amosov *et al*[34] used a SiO_2 glass; Bihuniak[35] used a type I glass, estimated according to impurity type and level; Doladugina & Lebedeva[36] used a KS4V glass; Hlavac & Sen[37] used a type I glass melted between 1050–1230°C; Leko & Gusakova[38] used a KU-1 glass and measured η at 1130°C; Leko & Meshcheryakova[39] used a KI type I glass; Orii *et al*[40] probably used a type I glass at 1200°C. All these authors measured the glass viscosity by the beam bending method. The fibre elongation method was used by Whitworth *et al*,[41] with a Vitreosil infrared glass at 1139°C; by Mackenzie,[42] that measured viscosity at 1228, 1276 and 1327°C; and by Yovanovitch,[43] that used a type I SiO_2 glass between 1000–1200°C. Bowen & Taylor[44] used a GE 124 glass and measured the viscosity by the falling ball method between 2085–2310°C. Clasen *et al*[45] performed viscosity measurements by the torsion method between 1480–1570°C; Donadieu *et al*[46] measured viscosity between 1000–1360°C, but these data were not considered here because they were obtained under a compressive stress of about 1 kbar. Dunn[47] made measurements by a concentric cylinder viscosimeter with tungsten crucible and spindle between 1810–2250°C, but did not disclose the specific glass type. Gusakova *et al*[48] used a KI glass melted from artificial quartz (type I) and made viscosity measurements by a rotating viscometer with Mo rotating body/crucible and also by the beam bending method [*]. Both techniques were also utilised by Leko *et al*,[75] that used some KI glasses from rock crystal made, artificial crystal [*] and synthetic cristobalite [**]; Leko *et al*[76] also measured η from natural quartz and other two estimated silica I types [*, **] between 1100–2000°C. Hoffmaier & Urbain[49] used a type I silica glass by melting in vacuum, and performed viscosity measurements by the compression method. Kimura[50] used a Vitreosil IR type I glass and measured viscosity by the beam bending and fibre elongation methods at 1100 and 1200°C. Loryan *et al*[51] used a type I glass and measured viscosity by penetration rotating methods between 1300–2000°C. A rotating viscosimeter was employed by Solomin,[52] that used a type I glass and measured η between 1720–2000°C; and by Urbain *et al*,[53] that probably used a type I glass and performed viscosity measurements in vacuum and argon atmospheres. Toshiba Ceramics Co.[54] researchers used a special T-2030 type I glass and measured η between 1097–1394°C. Weiss[55] used a Vitreosil IR and a GE 214 [*] type I glass using the torsion method in a wide temperature range. Brebec *et al*[85] used a commercial Puropsil A type I, with impurity content similar to Puropsil B, presented at Table 1.

For type II SiO_2 glass, the beam bending technique was applied by Amosov *et al*[34] using artificial quartz and gas flame; by Fontana & Plummer[56] (Armesil glass); by Mazurin & Klyuev[57] and by Leko *et al*,[75] that used a KU-2 glass and measured the viscosity between 1100–1300°C. Aslanova *et al*[33] probably used a type II (gas flame), and measured viscosity by the counterbalanced method in a Mo crucible. Bruckner[58] used a Homosil type II glass and the rotating viscosimeter with coaxial Ir cylinders (1686–2007°C). Bruisten & van Dam[59] and Clasen & Hermann[60] used Herasil III glass and measured η by the fibre elongation and torsion methods. Donadieu[61] probably used a type II SiO_2 glass. Gusakova *et al*[48] used a KU-2 type II glass, and measured viscosity by a rotating viscometer with a Mo rotating body and crucible and also with the beam bending method. Leko[62] used a type II silica glass with no indication of the measurement technique. Leko & Meshcheryakova[63] – and also in Leko *et al*[64] – probably used two different type II silica glasses, melted from glass flame and artificial quartz. The measurement of viscosity was carried out using the spring extension and beam-bending methods [*] between 1090–1176°C. Loryan *et al*[51] used a type II glass and measured viscosity by the penetration method between 1100–2000°C. Mazurin *et al*[65] probably used type II glasses from artificial quartz and from crystobalite [*], melted by glass flame method, and measured η by a rotating viscosimeter with Mo rotating body and crucible. Pavlova & Amatuni[66] used a KV type II glass with no indication of experimental procedure. Researchers at Toshiba Ceramics Co.[54] used a special T-1030 type II glass with no indication of the viscosity measurement method used between 1097–1394°C. Weiss[55] measured Herasil I, Vitreosil OG [*] and Ovisil 451

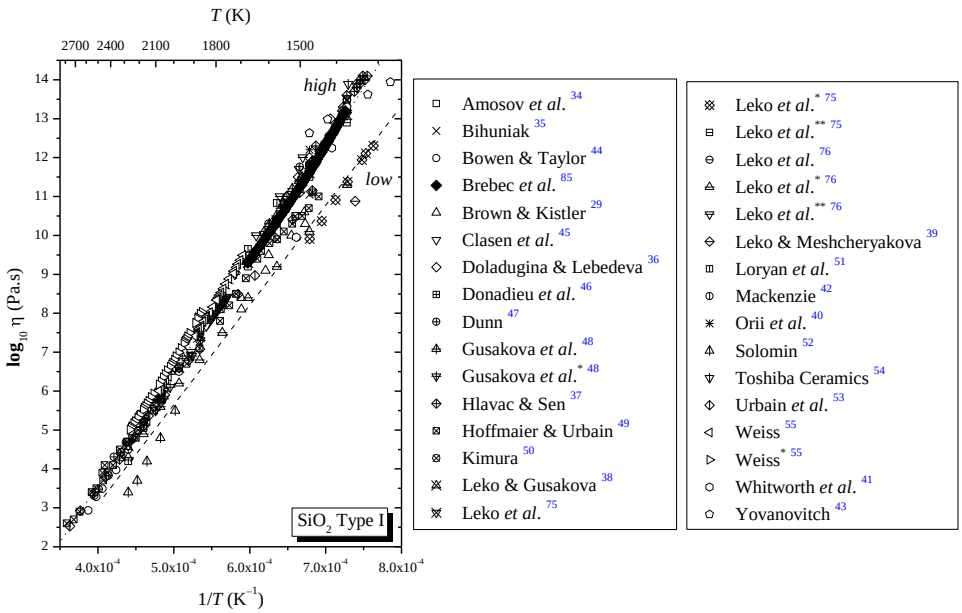

Figure 5. Viscosity data of type I silica glasses. The lines are Arrhenius fits and correspond to the highest (dotted) and lowest viscosities (dashed), see discussion

[**] type II SiO_2 glasses using the torsion method in wide temperature ranges.

For type III SiO_2 glass, Brown & Kistler[29] and Paek *et al*[67] (Suprasil II between 1895–2150°C) used the fibre elongation method. Hagy[68] (1099–1219°C), Mazurin *et al*[74] (1015–1250°C), Doladugina & Lebedeva[36] (1050–1200°C), Mazurin & Klyuev[57] (978–1125°C), Scherer[69] (1195–1275°C) and Schultz[70] (at 986 and 1064°C with a Corning 7940 glass) all applied the beam bending method. Gusakova *et al*[48] used a rotating viscometer using Mo rotating body/crucible and beam bending methods, 1080–1850°C, and a KU-1 type III glass. Kimura[50] used a Spectrosil glass and beam bending/fibre elongation methods at 1000, 1065 and 1100°C. Leko *et al*[75] used a KU-1 glass and beam bending and rotating methods for measurements between 1100–2000°C. Leko[62] presented no indication viscosity measurements, but measured between 1080–1940°C. Loryan *et al*[51] utilised the penetration and rotating methods between 1100–2000°C. Researchers at Toshiba Ceramics Co.[54] used a specially T-4040 type III glass measured between 1097–1394°C. Weiss[55] used Suprasil I and Synsil [*] type III silica glasses and the torsion method in a wide temperature range.

For type IV SiO_2 glass, Leko[62] and Leko & Gu-

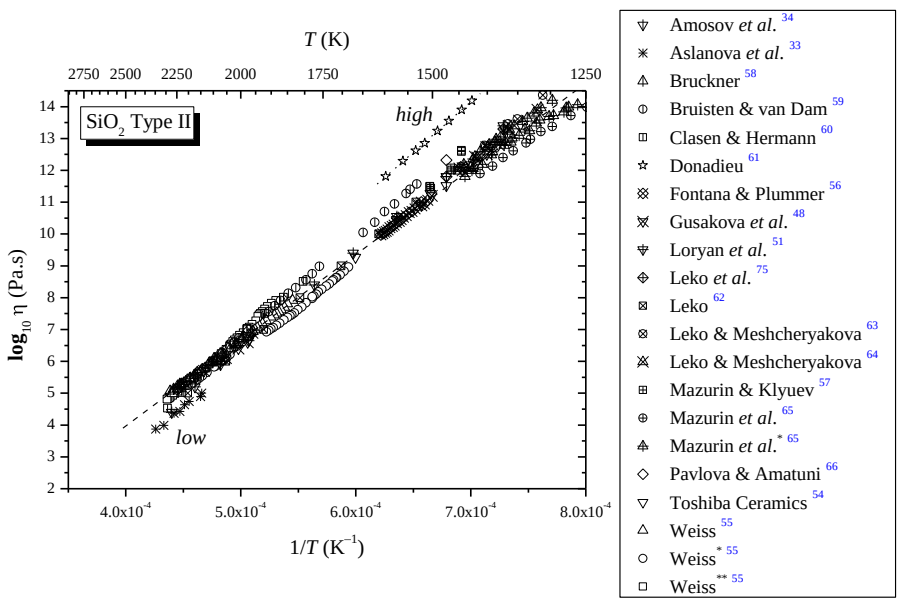

Figure 6. Viscosity data of type II silica glasses. The lines are Arrhenius fits that correspond to highest (dotted) and lowest viscosities (dashed) curves, see discussion

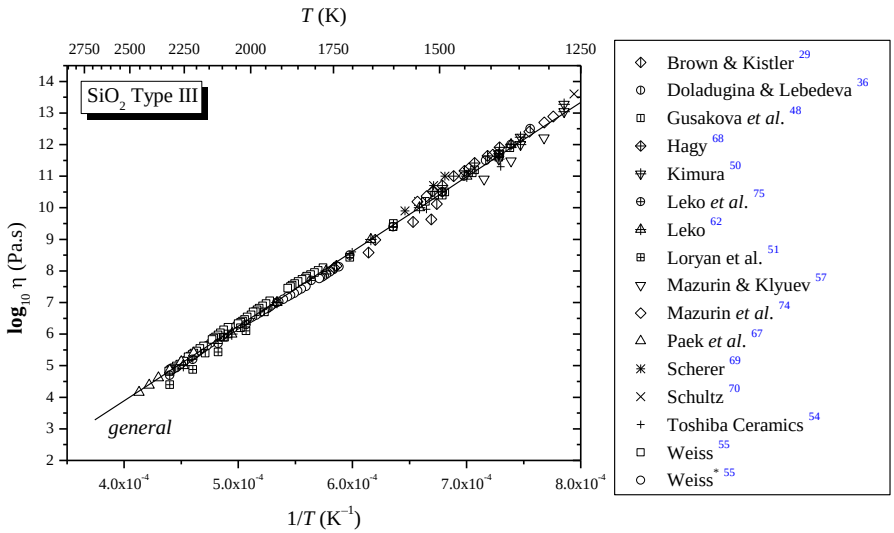

Figure 7. Viscosity data of type III silica glasses. The line is an Arrhenius fit corresponding to all experimental data denominated 'general'

sakova[77] probably used type IV silica glasses, but did not indicate the measurement procedure. The fibre elongation method was used by Ohashi *et al*[71] between 1295–1460°C. Shiraki *et al*[72] used the fibre drawing method, 1823–1980°C. Tajima *et al*[73] did not indicate the measurement procedure, but measured η between 1380–1450°C.

Figures 5–8 show that, as for the crystal growth rates, the viscosities of the different types of silica glasses[34–77] vary significantly and are strongly affected by impurities. Their effect is very similar in magnitude to that on the crystal growth rates. The lines shown on each graph correspond to an Arrhenius expression of the type: $\log_{10}\eta = A + B/T$, with η in Pa s, T in K. A and B are constants.

Figures 5 and 6 show several data sets for type I and type II silica glasses, respectively, but in our analysis we only considered the highest and the lowest viscosities. For type IV silica glass, Figure 8 shows that two data sets can be distinguished. Figure 7 shows an almost unique behaviour for all different glasses of type III. The variation of viscosity for this glass type is thus much smaller than that for the other silica glass types.

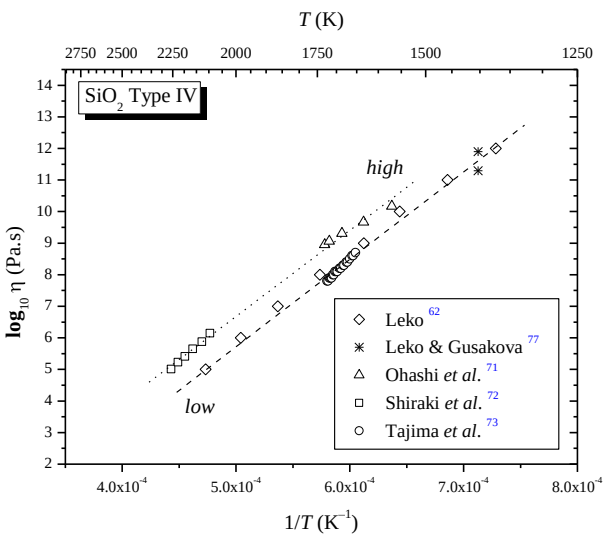

Figure 8. Viscosity data of type IV silica glasses. The lines are Arrhenius fits that correspond to the highest (dotted) and lowest viscosities (dashed) data, see discussion

5. Discussion

5.1. Analyses of crystal growth data

For all types of silica glasses, in the temperature range 1374–1420°C, we observed the following maximum variations of growth rates between the data of different authors: for type I=230× at T=1410°C; for type II=140× at T=1375°C; for type III=30× at T=1420°C; and for type IV=20× at T=1400°C. In other words, within each glass family there is a variation of crystal growth rates of one to two orders of magnitude.

Since the measurement of crystal growth rates is quite simple and the typical errors should not exceed 10–15%, this large scatter indicates that, for this particular system, u is very sensitive to the impurity content, which includes 'water' and chlorine. In particular, as expected, type I silicas (produced by melting of quartz and containing several impurities) presents a higher scatter of crystal growth rates than type III silicas (prepared from the hydrolysis of silicon compounds) or than type IV silicas (produced by $SiCl_4$ oxidation).

On can speculate that crystal growth kinetics are extremely dependent on the impurity level because the purest silica glasses have a fully polymerised network consisting of Q^4 unities (in NMR notation). The addition of impurities breaks some of the bridging Si–O–Si bonds, disrupting the continuous network and producing a distribution of Q^n (n=1, 2,

3) units that strongly affect transport phenomena, such as those focused here. The small concentration of impurities in type I silicas (for instance, circa 30 ppm alkali and 8 ppm OH^- in Puropsil B, as cited in Table 1) renders it very difficult to experimentally detect the corresponding small concentrations of Q^3 and Q^2, and possibly of Q^1 units. However, since the total content of (bond breaking) impurities is below ≈0·1% it is clear that the percentage of Q^4 units remains larger than ≈99·9% for most silica glasses.

5.2. Analyses of viscosity data

Similar differences are observed for viscosity, i.e. a scatter of about two orders of magnitude for silica types I and II; and one order of magnitude for silica types III and IV. For instance, taking T=1270°C and considering all types of silica glasses, the following variation of η is observed: 430× for type I; 100× for type II; 5× for type III; and 10× for type IV. Considering all the different sources/authors/techniques, there is thus a clear correspondence between the effect of impurities on the crystal growth rates and viscosities. It is clear that the glasses that present the slowest crystal growth rates and highest viscosities have fewer impurities.

That is why we combined the slowest crystal growth rates with the highest viscosities and *vice versa* in our kinetic analysis.

5.3. Crystal growth mechanism in silica types

For stoichiometric (polymorphic) crystallisation, as in the present case, short range molecular diffusion through the crystal/melt interface is expected to govern crystal growth. In most theoretical analyses of crystal growth kinetics in undercooled liquids, it is assumed that this type of molecular transport is determined by an effective diffusion coefficient, which is linked to the viscosity by the Eyring equation (Equation 2). With the assumption D_u=D_η, to analyse growth rate data one can thus insert Equation (2) into Equation (1), and use experimental values of $\eta(T)$, and $\Delta G(T)$ calculated by the Thomson equation, for instance.

However, the true size l (and the nature) of the diffusing atoms or 'building molecules' in Equations (1) and (2) is unknown. One can thus leave l as an adjustable parameter and fit Equation (1) to the growth rate data. For example, considering Wagstaff's growth rate data, Figure 1 shows a fitted growth rate curve, using the normal growth equation (Equation 1 with f=1) and D_η from the Eyring equation, which resulted in λ=2 Å (solid line, see details below).

In summary, each crystal growth curve in Figures 1–4 was linked to a given viscosity curve (from Figures 5–8) in a such a way that the fastest $u(T)$ was combined with the lowest $\eta(T)$ and *vice versa* for each glass type. For type III glass a single viscosity curve (denominated 'general') was used for all crystal growth rate data. The result is that, within some deviations, the normal growth mechanism describes the kinetics of the four types of silica glasses shown in Figures 1–4.

5.4. Arrhenius behaviour and activation energies for viscosity

Figures 5–8 show the viscosities of different silica glasses reported by several authors. Arrhenius lines $\log_{10}\eta$=A+B/T fit quite well the data of Figures 5–8 in wide temperature ranges.

Details of experimental data used were described above. The viscosity curves of the four types of silica glasses show Arrhenius-type behaviour, and glasses types I and II (having the lowest OH^- content) present the highest viscosities, activation energies of viscous flow, E_η, and T_g (curves denominated 'high' viscosity, dotted lines). In fact, the highest viscosity data for type I glass gives an activation energy for viscous flow E_η=569±5 kJ/mol, which is close to the experimental activation energy reported by Brebec *et al*[85] for Puropsil A glass (Type I): E_η=591±10 kJ/mol. The lowest viscosities are associated with the lowest activation energies for viscous flow and T_g. The exception is type IV glass, where the activation energy E_η of the glass having the highest viscosity is similar to that of the glass of lowest viscosity. Table 2 summarises the activation energies for viscous flow and T_g (considering $\log_{10}\eta(T_g)$=12 [in Pa s]) for the four silica glass types.

5.5. Link between viscosity and crystal growth rates

It is obvious that for a given glass type, the higher the viscosity the smaller the impurity content, highest activation energy for viscous flow, E_η, and highest T_g. Surprisingly, however, the viscosity of sixteen samples measured by different authors for type III glasses shows a variation of only half order of magnitude. As the growth rate, u, and viscosity, η, are inversely proportional (Equation (1)), similar findings were

Table 2. Approximate values of activation energies for viscous flow E_η *calculated from , and estimated* T_g *for each glass type and viscosity regime, according to Figures 5–8.*

Silica glass type	Viscosity curve	E_η (kJ/mol)	T_g (K)
Type I	lowest	490±13	1337
	highest	570±5	1606
Type II	lowest	520±4	1426
	highest	610±4	1583
Type III	general	450±2	1345
Type IV	lowest	530±4	1373
	highest	520±10	1438

observed for the crystal growth data of Figures 1–4. In fact, the influence of impurities on the magnitude of the viscosity is quite similar to that in the crystal growth rates in each glass type. The relatively small variations of viscosity for glass types III and IV are because they are made from synthetic chemicals and have the smallest variation of impurities, structural water and chlorine.

5.6. Glass transition temperatures of different silica glass types

The glass transition temperatures were measured for different silica glasses by a few authors, but, unfortunately, most did not indicate the glass types used. It should be stressed that experimental measurements by DSC or DTA are difficult with silica glass due to low variation of C_p. For instance, Mai *et al*: T_g=1495 K[81] (unknown measurement procedure and glass type); Nassau *et al*: T_g=1433 K[82] (by dilatometric measurement, but unknown glass type); Youngman *et al*: T_g=1459 K[83] (unknown type and measurement procedure). Another way to compare T_g was by using viscosity measurements, i.e. searching for the temperature where the viscosity is 10^{12} Pa s. The results shown in Table 2 are in agreement with measured T_g values. The purer the glass the higher is its T_g. Thus taking the highest viscosities, types I and II glasses have T_g values between 1583 and 1606 K, whereas T_g for types I and III glasses using lowest and general regimes, respectively, is between 1337 and 1345 K.

5.7. The melt/crystal interface temperature during crystallisation

Crystallisation is an exothermic process and knowledge of the melt/crystal interface temperature is essential in analysing crystal growth kinetics. Attempts to calculate the temperature distribution at the interface during crystal growth require many simplifying assumptions to solve this complex problem. However, from direct measurements for several glasses Herron and Bergeron[84] suggested an empirical equation to estimate the melt/crystal interface temperatures in six borates and one silicate glass ($Li_2O.2SiO_2$) based on experimental measurements, that were supposed to be valid around the maximum growth rate. Equation (4) was proposed by Herron & Bergeron for correcting of temperature of the interface at the maximum crystal growth u_{max}

$$\Delta T_i = 17{\cdot}12(u_{max}\Delta H_m)^{0{\cdot}486} \quad (4)$$

In Equation (4), ΔT_i is the temperature difference between the melt and the interface (°C), u_{max} is the maximum crystal growth rate (cm/s) and ΔH_m is the melt enthalpy (cal/cm^3). Equation (4) shows that interface temperature corrections for silica is ≈0·1°C.

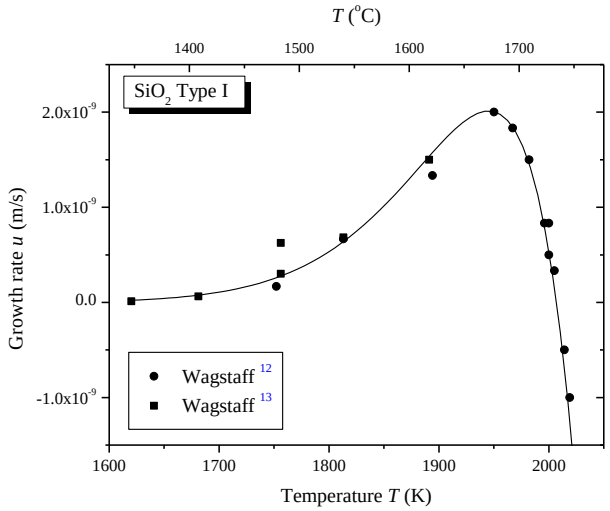

Figure 9. Normal growth model adjusted to Wagstaff's data for silica glass type I,[12–13] using Thomson's approximation for ΔG and the viscosity of Puropsil A.[86] The fitted jump distance is 2 Å

Thus, because of the low value of maximum crystal growth rate (compared to other oxide glasses) and low melting enthalpy, such correction was irrelevant for this particular glass.

5.8. Analysis of experimental results considering the normal growth model

From Equations (1) and (2), the expression for normal growth may be written as

$$u = f\frac{k_B T}{\lambda^2 \eta}\left[1-\exp\left(-|\Delta G|/RT\right)\right] \quad (5)$$

We assume f≈1, and η given by the Arrhenius equations fitted for each glass type (data sets from Figures 5–8). The normal growth model can be tested in two ways: first, using all the available data (Figures 1–4), taking some groups for which crystal growth kinetics are similar; or in fine detail for a relatively small undercooling range ΔT<380°C using only Wagstaff's data.[12–13] Thus, from all available crystal growth data from different sources, the fitted values of the jumping distance, λ, were approximately 1 Å. It would be ideal to use the crystal growth rates and viscosity from samples obtained from the same batch to avoid the influence of impurities, but this was not feasible here. It was, however, possible to use data for same silica types, combining the lowest viscosities with the highest growth rates and *vice versa*.

Wagstaff[12] studied the temperature dependence of the fraction of preferred growth sites on the crystal/glass interface, f. At low undercoolings a plot of $u_R = u\eta/[1-\exp(-|\Delta G|/RT)]$ versus ΔT should yield a straight line parallel to the x-axis,[1,12] and this indeed was observed. Thus, this appears to be the operative mechanism in this system. This type of analysis us-

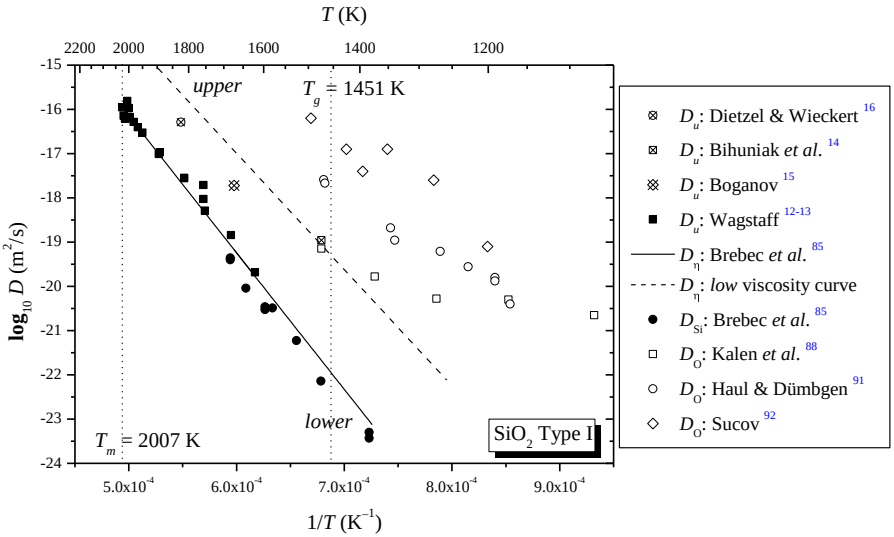

Figure 10. Logarithm of effective diffusion coefficients in type I silica glasses: D_u: calculated here from the crystal growth rate data of Wagstaff,[12,13] Boganov,[15] Dietzel & Wieckert[16] and Bihuniak et al.[35] *using Equation 6 corresponding to the slowest and fastest bounds of Figure 1; D_η: Diffusion coefficients calculated by the Eyring equation (Equation 2). Solid line: using the viscosity data for Puropsil A silica[85] with λ=2 Å. These diffusivities correspond to the highest viscosity curve of Figure 5, or lower diffusion limit; Dashed line: using the lowest viscosity curve of Figure 5 with λ=0·16 Å, the upper diffusion limit; D_{Si} and D_O: Measured self-diffusion coefficients of Si^{4+}[85] and O^{2-}[88,91,92] (see respective symbols in the insert); dotted lines corresponds to melting (T_m) - as experimentally observed by Wagstaff[12,13] - and T_g temperatures of Puropsil A, respectively (see text for more details)*

ing u_R was performed in almost all previous crystal growth studies, because this procedure does not need the use of the jumping distance λ.

Figure 9 shows that the normal growth model fits quite well Wagstaff's data. Fitting with a Levenberg–Marquardt nonlinear algorithm resulted in a correlation factor R^2=0·96. The fitting parameter was the jump distance. All the other parameters: melting enthalpy ΔH_m, melting point T_m and viscosity $\eta(T)$, were independently measured. These values were presented by Wagstaff (ΔH_m=7680 J/mol; T_m≈2007 K, viscosity from Brebec *et al*[85] (Puropsil A glass): $\log_{10}\eta$=−8·81166+30193·77/T (η in Pa s, T in K). The resulting fitted value of λ=2 Å is close to the average Si–O bond length (1·59 Å) in silicate glasses,[86] and about 2·5 times higher than the ionic Si^{4+} diameter (0·8 Å), but somewhat lower than the O^{2-} (2·7 Å) and is thus an acceptable value. We should stress that from such fitting of crystal growth rates one cannot calculate the exact value of the jump distance. Therefore only the order of magnitude for the size of the 'structural units' involved in crystallisation is obtained because the fitted λ values carry all the errors related to the uncertainties in the other parameters of the normal crystal growth model.

5.9. Activation energies and diffusivities in bulk silica glasses

In most theoretical analysis of crystal growth kinetics in undercooled melts it is assumed that short range molecular transport through the crystal/melt interface is determined by the diffusivity of the slowest species. It is also assumed that the effective diffusion coefficient of such species can be calculated via the viscosity, η, by means of the Eyring expression (Equation (2)). This expression thus relates viscosity and diffusivity, D_η, of the rate determining flow unities. However, it has been a matter of discussion if Equation (2) could be used for such calculations at deep undercoolings, near T_g, (e.g. see discussions in Nascimento *et al*[10]). Our aim here is to compare diffusion coefficients calculated from crystal growth rate data, D_u, from about T_m to ≈1·2 T_g, with those calculated through viscosity, D_η, and with directly measured diffusion coefficients of silicon and oxygen (when available) for each glass type.

Since we now know the governing growth mechanism in silica glass, let us analyse the diffusion coefficients in more detail. For normal growth one can isolate an effective diffusion coefficient, D_u, from Equation (1), as shown by Equation (6)

$$D_u = u\lambda\left[1-\exp\left(-\frac{|\Delta G|}{RT}\right)\right]^{-1} \qquad (6)$$

This parameter can be estimated using the experimental growth rate data and λ from the previous fits for each glass type. The combination of the slowest crystal growth rates with the highest viscosities (and *vice versa*) thus yields D_u for each silica glass type.

Figures 10–13 show a good agreement between D_u and D_η for all four glass types. In addition, the calcu-

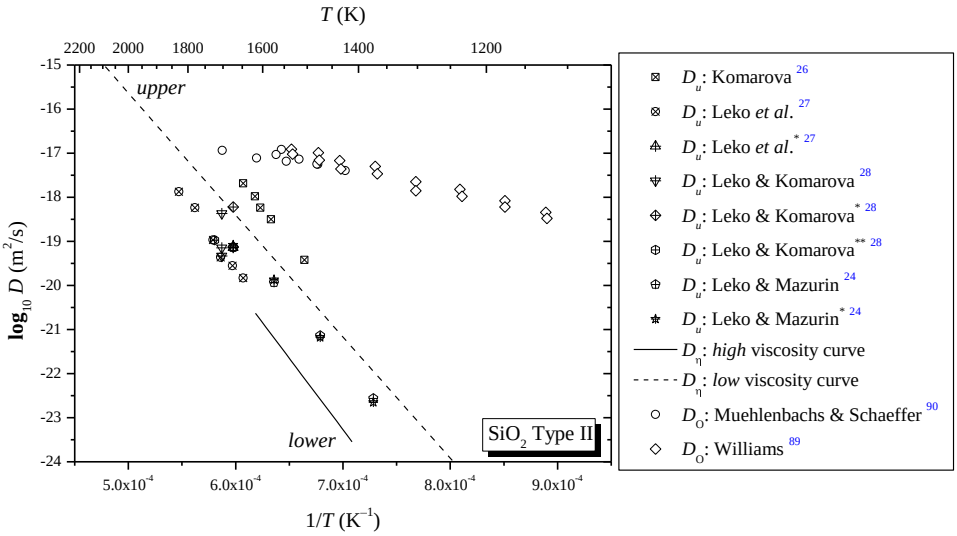

Figure 11. Logarithm of effective diffusion coefficients in type II silica glasses: D_u*: calculated from crystal growth rate data of Leko & Mazurin,*[24,64] *Komarova,*[26] *Leko* et al.[27] *and Leko & Komarova*[28] *using Equation (6) corresponding to the slower and faster bounds of Figure 2;* D_η*: Diffusion coefficients calculated by the Eyring equation (Equation (2)). Solid line: using the highest viscosity data of Figure 6, the lower limit for diffusion. Dashed line: using the lowest viscosity data of Figure 6, the upper diffusion limit; both with* λ*=0·26 Å;* D_O*: Measured self-diffusion coefficients of* O^{2-}[89,90] *(see respective symbols in the insert)*

lated solid and dashed lines (D_η) correctly describe the temperature dependence of D_u. These effective diffusivities, D_η, calculated via viscosity and D_u from crystal growth rates, could be seen as *upper* and *lower bounds* for each silica type (Figures 10–13), with a difference of about one order of magnitude, but similar temperature dependences. In summary, the congruence of D_u and D_η indicates that, whatever the bond breaking and molecular reorientation mechanism required for crystallisation is, it is the same as that required for the atomic transport mechanism that controls viscous flow.

5.10. Silicon and oxygen diffusion in different types of silica glasses

Figure 10 shows experimental values of oxygen (O^{2-}) and silicon (Si^{4+}) diffusivities of type I silica glass in undercooled liquid silica[85,87–93] between 1073 and 1703 K. Figures 11–12 present oxygen diffusivities

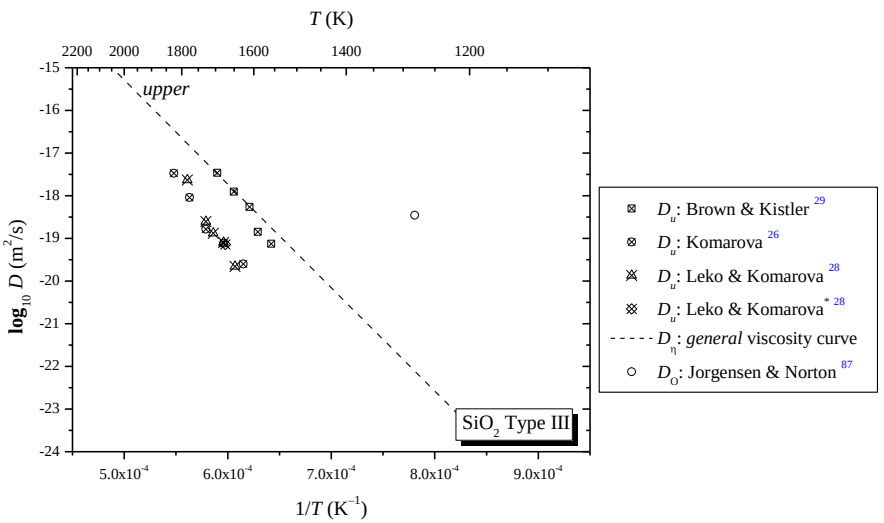

Figure 12. Logarithm of diffusion coefficients in type III silica glasses: D_u*: calculated from crystal growth rate data of Komarova,*[26] *Leko & Komarova*[28] *and Brown & Kistler*[29] *via Equation 6 corresponding to the slowest and fastest bounds of Figure 3;* D_η*: Diffusion coefficient calculated by the Eyring equation (Equation 2). Dashed line: using the 'general' viscosity data of Figure 7 with* λ*=0·3 Å, that could be due to no impurity influence and indicates an upper limit for diffusion. The lower bound refers to* D_u *calculated form data from Komarova e Leko & Komarova (see symbols).* D_O*: Measured self-diffusion coefficient of* O^{2-}[87] *(see respective symbol in the insert)*

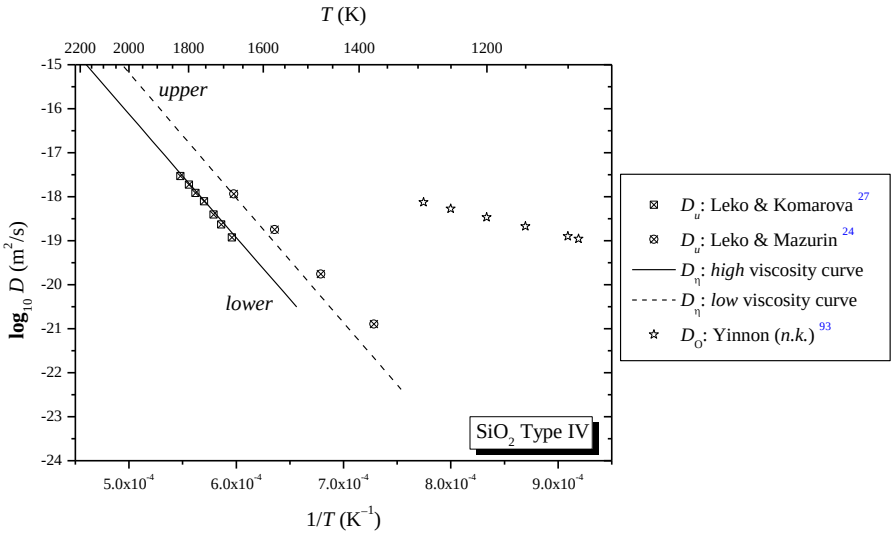

Figure 13. Logarithm of diffusion coefficients in type IV silica glasses: D_u*: calculated from Leko & Mazurin*[24] *and Leko & Komarova*[27] *crystal growth rate data (Equation (6)) corresponding to the slowest and fastest bounds of Figure 4;* D_η*: Diffusion coefficients calculated by the Eyring equation (Equation 2). Solid line: using the highest viscosity data of Figure 8 with λ=0·77 Å, that indicates the lower limit for diffusion. Dashed line: uses the lowest viscosity data of Figure 8, with λ=0·8 Å, and indicates the upper limit.* D_O*: Measured self-diffusion coefficient of* O^{2-} *in undetermined silica type*[93] *(see respective symbols in the insert); n.k.: unidentified vitreous silica type*

corresponding to glass types II and III, respectively. As far as we know, there are no diffusion measurements for type IV silica. Figure 13 shows Yinnon's data[93] for oxygen diffusivity in an unknown silica type, just for comparison. An analysis of oxygen self diffusion in SiO_2 glass reveals a large scatter of activation energies and pre-exponential factors (Figures 10–13).

For type I silica glass D_O clearly differs from D_u and D_η, (but D_{Si} is equal to D_u and D_η). Schaeffer[94] suggested that the activation energy for oxygen self diffusion in silica glass is close to 100 kJ/mol, much less than the single bond strength between silicon and oxygen (465 kJ/mol). Our review of oxygen tracer diffusion in SiO_2 glass reveals a larger scatter of activation energies (100–300 kJ/mol) and pre-exponential factors (according to Table 3), but these values are well below 465 kJ/mol and confirm Schaeffer's findings.

By analogy with crystal growth rates and viscosities, the most important causes for the differences in oxygen diffusion rates in different samples (shown in Figures 10–13) are quite likely variations in impurity content. But, according to Table 3, even for the same glass (Armesil, type II) there are some significant differences in the activation energies obtained from different techniques. Thus experimental errors from the different techniques employed in each work may also partially explain these discrepant values. On the other hand, it is absolutely clear from Figures 10–13 that, despite the scatter, the oxygen diffusion coefficients are several orders of magnitude *higher* than those of silicon, and that their temperature dependence (activation energy) are smaller than that for silicon diffusion.

It is not trivial to separately characterise transport of oxygen in different chemical forms. However, recently Kajihara *et al*[95] distinguished diffusion of molecular oxygen (O_2) from other oxygen species in silica glasses using photoluminescence. Their results were compared with the oxygen permeation data of Norton[96] and of Hetherington & Jack.[97] The diffusivity of molecular oxygen from these three sources are more than five orders of magnitude larger than those reported in our Figures 10–14 for ionic oxygen. These slow diffusivities have been attributed to hopping of oxygen ions belonging to the silica glass lattice. On the other hand, the structure of SiO_2 glass is relatively open allowing the incorporation of molecular O_2 without a significant interaction with the silica lattice; and thus oxygen molecules (O_2) have much higher diffusivities than oxygen ions. We are not dealing with molecular oxygen here, but the above discussion indicates that different oxygen types have widely different mobilities. An important note is that there is more agreement between molecular oxygen diffusivities from different authors than for the BO/NBO oxygen diffusivities (and this finding is understandable if one considers varying Q^n amounts according to the impurities in each glass, as explained below). Therefore impurities do not significantly change molecular oxygen diffusivities, but have a strong role on ionic oxygen diffusion, and this type of diffusion is of primary interest to this paper.

Type I is the unique silica glass for which there are reported data for silicon self diffusion. It is ex-

Table 3. Pre-exponential diffusivities (D_0) and activation energies (E_A) of different vitreous silica types: determined by different methods for the glasses shown in Figures 10–14. Oxygen data for bulk glasses;[87–93] silicon data for bulk glass;[85] oxygen data for thin films,[98–102] and silicon data for thin films.[103–106] In parenthesis we list the commercial brand name (n.k.: not known). [*] Jorgensen & Norton, and Costello & Tresller measured oxygen diffusivities only at one temperature (here established as D_0), as indicated ϑ

Glass type	*Diffusivity type*	*Method*	*ΔT range (K)*	D_0 *(m^2/s)*	E_A *(kJ/mol)*
I (n.k.)	D_u : Wagstaff, Equation (6)	From crystal growth	1623–2007	$1{\cdot}4\times10^{-2}$	547±18
I (Puropsil A)	D_η : Eyring relation, Equation (2)	From viscosity	1373–1673	$1{\cdot}8\times10^{-1}$	591±1
I (Puropsil A)	DSi : Brebec *et al*	SIMS	1383–683	$1{\cdot}3\times10^{-3}$	579±14
I (GE 124)	DO: Kalen *et al*	SIMS	1073–1473	$5{\cdot}5\times10^{-15}$	143±24
I (Heraeus)	DO: Haul & Dümbgen	Rate uptake	1173–1523	$4{\cdot}3\times10^{-10}$	234±18
I (n.k.)	Sucov	Tracer loss	1198–1498	$1{\cdot}5\times10^{-6}$	298±22
II (Amersil)	DO: Muehlenbachs & Schaeffer	Rate of exchange	1423–1703	$4{\cdot}4\times10^{-15}$	82±17
II (Amersil)	DO: Williams	Rate uptake	1123–1523	$2{\cdot}0\times10^{-13}$	121±8
III (n.k.)	DO: Jorgensen & Norton [*]	(n.i.)	1281	$3{\cdot}5\times10^{-19}$	-
(n.k.)	DO: Yinnon	NRA	1088–1291	$2{\cdot}1\times10^{-14}$	110
Thin film	DO: Mikkelsen	SIMS	1473–1673	$2{\cdot}6\times10^{-4}$	454±30
Thin film	DO: Cawley & Boyce	SIMS	1173–1473	$2{\cdot}8\times10^{-9}$	280±10
Thin film	DO: Pfeffer & Ohring	Tracer (room air)	673–1073	$1{\cdot}3\times10^{-16}$	64·8±5·8
Thin film	DO: Costello & Tresller [*]	SIMS	1273	4×10^{-15}	-
Thin film	DSi: Takahashi *et al* (1% partial pressure)	SIMS	1423–1573	8×10^{-5}	502±77
Thin film	DSi: Mathiot *et al*	SIMS	1273–1473	$3{\cdot}2\times10^{-3}$	515
Thin film	DSi: Tsoukalas, Tsamis & Stoemenos	SIMS	1323–1373	$3{\cdot}7\times10^{-6}$	405
Thin film	DSi: Tsoukalas, Tsamis & Normand	SIMS	1323–1423	$1{\cdot}2\times10^{-4}$	457±24

tremely difficult to obtain very sluggish diffusion coefficients such as those of Table 3, but Brebec *et al*[85] managed to measure Si^{4+} diffusion in silica glass using SIMS (secondary ion mass spectroscopy). The activation energy for Si^{4+} diffusion in SiO_2 glass (Type I, Puropsil A) is about 580 kJ/mol in the temperature range between 1413–1683 K. According to Figure 10, diffusivity calculated from crystal growth rate (D_u) correlates very well with the values calculated from viscosity (D_η). In addition, the activation energies for viscous flow (Table 2) are close to the activation energy for silicon diffusion. In fact, the coincidence of the activation energies for viscous flow and crystal growth with those calculated from self diffusion of silicon, but not of oxygen, suggests that Si and O do not diffuse together, at the same rate, during crystal growth.

Since silicon and bridging oxygens (BO=Si–O–Si) are tightly linked, one might argue why the diffusivities of these two network building species are so different? A reasonable explanation is that Si and O do not diffuse together at the same rate; or when one measures oxygen diffusivity in silica, in reality only the movement of nonbridging oxygens (NBO=Si–O–M, where M refer to impurity elements in the glass), which are not so tightly bound to the silicon tetrahedra, are being measured because NBO can move much faster than BO. This proposal is consistent with the conclusions of Kalen *et al*,[88] that considered the scatter shown in Table 3 be qualitatively explained by the existence of at least two mechanisms for oxygen ion diffusion: network and interstitial.

In an ideal, 100% pure silica glass having no impurities, only Q^4 units should exist. In this case one should expect that Si and O would have similar diffusivities. For real glasses, several diffusivity data would be ideally compared considering a single glass from the same batch (having exactly same impurity content and consequently the same BO/NBO fraction), as we present in this paper for Puropsil A. In Figure 10 the diffusivities and activation energies for silicon diffusion and viscous flow of Puropsil A are indeed quite close.

An ideal experiment would be one with the four types of diffusivities determined from the same glass samples and in the same temperature range, but unfortunately such data are not available. We were thus careful to choose data for glasses of the same type, supposedly having similar impurity contents; and the values of D_η, D_u and D_{Si} are indeed coherent. For Puropsil A glass (i.e. samples from the same batch) viscosity diffusion, D_η, and Si diffusion, D_{Si}, agree, as shown in Figure 10, up to below T_g (considering the same batch). This finding confirms that viscous flow and crystal growth are controlled by silicon diffusion in undercooled silica.

5.11. Activation energies and diffusivities in thin film silica glasses

For the sake of completeness we also discuss available diffusion data for thin film silica glass although we could not find viscosity and crystal growth data.

Figure 14 shows diffusivity measurements of silicon and oxygen in thin film silicas, under different conditions. One notes that D_O and D_{Si} follow different patterns, as we previously observed for bulk silica glasses. Table 3 also shows the pre-exponentials, diffusivities and activation energies for these systems. The activation energies for Si diffusion are higher than those of oxygen.

Mikkelsen,[98] compared his results for oxygen dif-

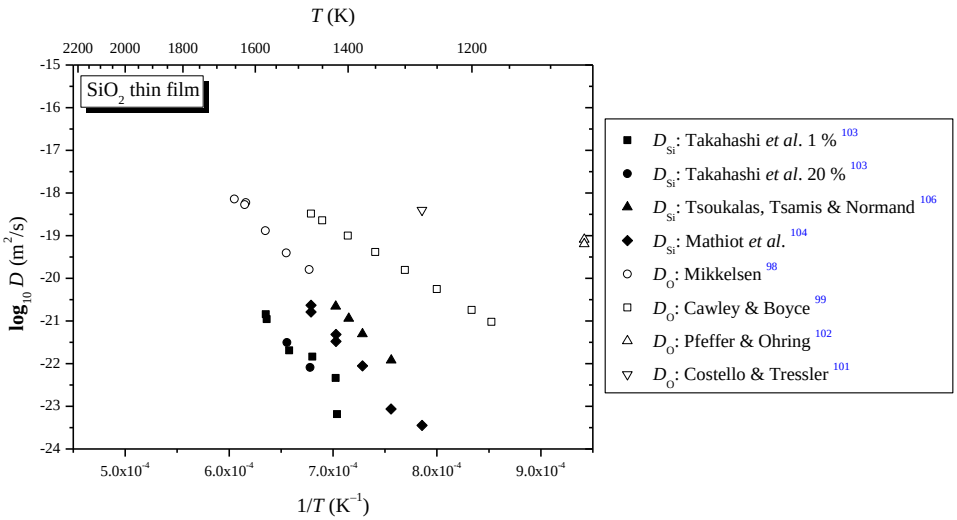

Figure 14. Self diffusion coefficients of Si and O in thin film silicas: D_{Si}*: Measured self diffusion coefficients of silicon (closed symbols): Sources: Takahashi* et al[103] *(measurements at 1 and 20% oxygen partial pressure), Mathiot* et al[104] *and Tsoukalas* et al[105,106] D_O*: Measured self diffusion coefficients of oxygen (open symbols). Sources: Mikkelsen,*[98] *Cawley & Boyce,*[99] *Costello & Tressler* [101] *and Pfeffer & Ohring.*[102] *Oxygen diffusion is faster than silicon diffusion in all cases except one*

fusivities in thin films with those determined by Haul and Dümbgen[91] for bulk silica, and found them to be 10 to 100 times lower (with activation energy of 454 kJ/mol between 1473–1673 K). Obviously, considering the previous discussions for bulk silica glasses, impurity effects should have been considered. Mikkelsen[98] assumed that his results represent a limit for the intrinsic network oxygen (bridging oxygen) diffusivity in silica glass. It is also important to note the comparison of results of Mikkelsen[98] [E_O=454±30 kJ/mol, D_0=2·6×10^{-4} m^2/s between 1473–1653 K] and Cawley & Boyle[99] [E_O=280±10 kJ/mol, D_0=2·8×10^{-9} m^2/s between 1173–1473 K] in Table 3. They used the same technique (SIMS) and observed different results for the diffusivities and activation energies. The explanation for such discrepancy probably reflects different impurity contents.

Unfortunately, the impurity content was not given in most thin film papers. Ham & Helms[100] pointed out that their 'slow' diffusion rates for ionic oxygen agree with Mikkelsen's, but disagree from Costello & Tressler's.[101] Oxygen diffusivity measurements of Pfeffer & Ohring[102] at temperatures below 1423 K in air showed similar results as Costello & Tressler's. Ham & Helms believe that this discrepancy in diffusivities arises from 'drier' conditions. Costello & Tressler[101] did not report the concentration of water in their experiment, but a numerical simulation of water exchange during diffusion done by Ham & Helms suggests that 100 ppm water produced the same profiles, what is a typical value for the water content in bulk silica glass type I (Table 1).

From all silicon diffusivities measured in thin films, only those of Takahashi *et al*[103] match the diffusivities and activation energies measured by Brebec *et al*[85] for bulk silica. Data from Mathiot *et al*[104] lie within one order of magnitude to those of Takahashi *et al* and those of Brebec *et al.* The diffusivities measured by Takahashi *et al* did not depend on the oxygen partial pressure (1 or 20%). All other silicon results are more than two orders of magnitude higher, and almost all refer to non-stoichiometric compositions (unfortunately, without chemical analysis; more details see Tsoukalas *et al*[105, 106]). This interpretation is supported by the low activation energies found,[105,106] the difference arising from the defect formation energies of the mediating silicon self diffusion.

One could thus consider some of these data[104,106] as an upper bound of silicon self diffusion. Thus, following similar procedure from Figures 10–13, the silicon diffusivities of Takahashi *et al*[103] and Tsoukalas *et al*[106] in Figure 14 could be viewed as lower and upper limits for silicon diffusion in thin films, respectively.

One important note is that the oxygen data of Mikkelsen[98] (the smallest values for this anion) are similar to the upper limit of silicon diffusion. We speculate here that this result is a mere coincidence because all the several other data for silicon and oxygen indicates that the first diffuses much slower than the second in this glass.

In any case, it is clear that impurities extremely alter the diffusivity of any ion in a glass former such as silica (in bulk form or thin film), and thus small variations in impurity content could explain the scatter of oxygen diffusivities in Figures 10–14, even for the same silica type. But considering the same silica type, experimental data on diffusivities D_u, D_η and D_O (when applicable) are well defined, within upper or lower limits in bulk silica or thin films.

In summary, the close similarity of the activation energies and diffusivities determined in three independent ways: silicon self diffusion, viscous flow, and crystal growth indicates that the required bond breaking and molecular reorientation is comparable for these three kinetic processes. In particular it should be emphasized that there is no sign of decoupling between D_η and D_{Si} down to T_g. This similarity ensures that viscosity data may be used to estimate crystal growth rates in silica glasses. The present results provide a better understanding of the dynamics of transport processes in undercooled silica. But it will be important to perform similar analyses from T_m to about T_g for other glass forming silicate liquids to ascertain whether or not the present findings can be generalised.

6. Conclusions

To understand the dynamics of several processes in undercooled liquid silica, which is an archetypical network glass former, has been of long standing interest. Here we performed a critical analysis of a plethora of data for silicon and oxygen self-diffusion, viscous flow, and crystal growth kinetics in different types of commercial silica glasses and thin films, in a wide temperature range, from circa T_g to T_m, which led us to the following conclusions:

i. Crystal growth rates, oxygen self diffusion, and viscous flow in this particular system strongly depend on the impurity level, much more than in multicomponent silicate glasses. For each silica glass type, the variations of crystal growth rates between different glass batches (measured by different authors) correspond to similar variations observed for viscosity. This sensitivity is due to the fact that the purest silica glass has a fully polymerised network (Q^4) that is readily disrupted by small amounts of modifier impurity cations.

ii. We confirmed that normal growth is the operative mechanism of crystal growth in the four types of bulk silica glasses analysed, in broad temperature ranges. The calculated jump distance λ is about 0·2–2·0 Å, for the different types of silica glasses, and these values are of the (expected) order of magnitude of the Si–O distance.

iii. for type I silica glass, the activation energies for viscous flow (590 kJ/mol), crystal growth (550 kJ/mol) and silicon self diffusion (580 kJ/mol) are equal within experimental error. But the value for oxygen self diffusion is less than half (100–300 kJ/mol). Thus there is no decoupling between, D_u , D_η and D_{Si} and silicon controls the transport mechanism involved in crystal growth and viscous flow in this glass.

iv. The congruence of D_u and D_η in all four silica types indicates that the bond breaking and molecular reorientation mechanism required for crystallisation is the same required for the atomic transport mechanism that controls viscous flow. Then, viscosity data can be used to estimate the transport part that controls crystal growth in this glass from the melting point down to T_g.

This work with highly polymerised silica glass corroborates a previous analysis carried out for depolymerised diopside glasses and thus provides a step forward in the knowledge of kinetic processes controlling crystal growth in undercooled silicate liquids.

Acknowledgements

Special thanks to V. M. Fokin (Vavilov State Optical Institute, Russia), J. W. P. Schmelzer (University of Rostock, Germany) and G. P. Souza (UFSCar, Brazil) for reviewing this manuscript. Financial support from Brazilian agencies CAPES, CNPq, and FAPESP are fully appreciated.

References

1. Gutzow, I. In *Crystal Growth and Materials*. Edited by E. Kaldis & H. J. Scheel, North-Holland, Amsterdam, 1977.
2. Uhlmann, D. R., Uhlmann, E. V. & Weinberg, M. C. *Nucleation and Crystallisation in Liquids and Glasses*. The American Ceramic Society, Westerville-OH, 1993.
3. Vogel, W. *Glass Chemistry*. Springer-Verlag, Berlin, 1994.
4. Gutzow, I. & Schmelzer, J. W. P. *The Vitreous State*. Springer, Berlin, 1995.
5. Hölland, W. & Beall, G. *Glass Ceramic Technology*. The American Ceramic Society, Westerville, OH, 2002.
6. Vergano, P. J. & Uhlmann, D. R. *Phys. Chem. Glasses*, 1970, **11** (2), 39–45.
7. Meiling, G. S. & Uhlmann, D. R. *Phys. Chem. Glasses*, 1967, **8** (2), 62–3.
8. Leedecke, C. J. & Bergeron, C. G. *J. Cryst. Growth*, 1976, **32**, 327.
9. Burgner, L. L. & Weinberg, M. C. *J. Non-Cryst. Solids*, 2001, **279**, 28.
10. Nascimento, M. L. F., Ferreira, E. B. & Zanotto, E. D. *J. Chem. Phys.*, 2004, **121**, 8924.
11. Reinsch, S., Müller, R., Nascimento, M. L. F. & Zanotto, E. D. *Proc. XX ICG*, Kyoto, 2004.
12. Wagstaff, F. E. *J. Am. Ceram. Soc.*, 1969, **52**, 650.
13. Wagstaff, F. E. *J. Am. Ceram. Soc.*, 1968, **51**, 449.
14. Bihuniak, P. P., Calabrese, A. & Erwin, E. M. *J. Am. Ceram. Soc.*, 1983, **66**, C134.
15. Boganov, A. G., Rudenko, V. S. & Cheremisin, I. I. *Proc. X Intern. Congr. on Glass*, 1974, Kyoto. P. 66.
16. Dietzel, A. & Wickert, H. *Glastech. Ber.*, 1956, **29**, 1.
17. Hlavac, J. & Vaskova, L. *Silikaty*, 1965, **9**, 237.
18. Komarova, L. A. & Leko, V. K. *Elektrotekhn. Prom., Ser. Svetotekhn. Izdel.*, 1975, **1**, 2.
19. Leko, V. K. & Komarova, L. A. *Neorg. Mater.*, 1971, **7**, 2240.
20. Leko, V. K. & Komarova, L. A. *Neorg. Mater.*, 1975, **11**, 2106.
21. Leko, V. K. & Komarova, L. A. *Neorg.Mater.*, 1975, **11**, 1864.
22. Leko, V. K. Komarova, L. A. & Mazurin, O. V. *Neorg. Mater.*, 1972, **8**, 1125.
23. Leko, V. K. &Komarova, L. A. *Fiz. Khim. Stekla*, 1975, **1**, 335.
24. Leko, V. K. & Mazurin, O. V. *Svoistva Kvartsevogo Stekla*. Nauka. Leningrad, 1985.
25. Vaskova, L. & Hlavac, J. *Silikaty*, 1969, **13**, 211.
26. Komarova, L. A. *PhD Thesis*. 1973. Leningrad.
27. Leko, V. K., Komarova, L. A. & Mazurin, O. V. *Silikattechnik* 1974, **25**, 81.
28. Leko, V. K. & Komarova, L. A. *Neorg.Mater.*, 1974, **10**, 1872.
29. Brown, S. D. & Kistler, S. S. *J. Am. Ceram. Soc.*, 1959, **42**, 263.
30. Mazurin, O. V., Leko, V. K. & Komarova, L. A. *J. Non-Cryst. Solids,*

1975, **18**, 1.
31. Pavlova, G. A., Leko, V. K. & Komarova, L. A. *Fiz. Khim. Stekla,* 1975, **1**, 149.
32. Leko, V. K. & Komarova, L. A. *Neorg. Mater*., 1975, **11**, 1115.
33. Aslanova, M. S., Chernov, V. A. & Kulakov, L. F. *Steklo Keram*., 1974, **6**, 19.
34. Amosov, A. V., Leko, V. K. & Meshcheryakova, E. V. *Fiz. Khim. Stekla,* 1978, **4**, 416.
35. Bihuniak, P. P. *J. Am. Ceram. Soc*., 1983, **66**, C188.
36. Doladugina, V. S. & Lebedeva, R. B. *Fiz. Khim. Stekla,* 1993, **19**, 49.
37. Hlavac, J. & Sen, T. K. *Silikaty,* 1968, **12**, 213.
38. Leko, V. K. & Gusakova, N. K. *Fiz. Khim. Stekla,* 1977, **3**, 226.
39. Leko, V. K. & Meshcheryakova, E. V. *Fiz. Khim. Stekla,* 1975, **1**, 264.
40. Orii, K., Hara, Y., Akiyama, T., Tsukuma, K. & Kikuchi, Y. *Ceram. Abstr*., 1997, **76**, 30.
41. Whitworth, C. R., Bunnell, L. & Brown, S. D. In: *Front. Glass Sci. Technol*., Sheffield, 1970, P. 87.
42. Mackenzie, J. D. *Phys. Chem. Glasses,* 1962, **3** (2), 50–3.
43. Yovanovitch, J. *C. R. Acad. Sci.* (*Compt. Rend*.), 1961, **253**, 853.
44. Bowen, D. W. & Taylor, R. W. *Am. Ceram. Soc. Bull*., 1978, **57**, 818.
45. Clasen, R., Hornfeck, M. & Rosenbaum, S. *Proc. XVII Int. Congr. on Glass. Beijing, 1995*, **Vol. 5**, 181.
46. Donadieu, P., Jaoul, O. & Kleman, M. *Philos. Mag. A,* 1985, **52**, 5.
47. Dunn, S. A. *Am. Ceram. Soc. Bull*., 1968, **47**, 554.
48. Gusakova, N. K., Leko, V. K., Meshcheryakova, E. V. & Lebedeva, R. B. *Neorg. Mater*., 1974, **10**, 338.
49. Hofmaier, G. & Urbain, G. *Sci. Ceram*., 1968, **4**, 25.
50. Kimura, T. *Jpn. J. Appl. Phys*., 1969, **8**, 1397.
51. Loryan, S. G., Kostanyan, K. A., Saringyulyan, R. S., Kafyrov, V. M. & Bagdasaryan, E. Kh. *Elektron. Tekh. Ser.6, Mater*., 1976, **2**, 53.
52. Solomin, N. V. *Zh. Fiz. Khim*., 1940, **14**, 235.
53. Urbain, G., Bottinga, Y. & Richet, P. *Geochim. Cosmochim. Acta,* 1982, 46,1061.
54. Toshiba Ceramics Co., *Quartz Glass and Silica Glass*, 1979, Tokyo.
55. Weiss, W. *J. Am. Ceram. Soc*., 1984, **67**, 213.
56. Fontana, E. H. & Plummer, W. A. *Phys. Chem. Glasses,* 1966, 7 (4), 139–46.
57. Mazurin, O. V. & Klyuev, V. P. *Neorg. Mater*., 1974, **10**, 1115.
58. Bruckner, R. *Glastech. Ber*., 1964, **37**, 413.
59. Bruisten, P. M. & van Dam, H. B. B. *Proc. First Int. Conf. Fundamentals of Glass Manufacturing Process*. Sheffield, 1991, P. 18.
60. Clasen, R. & Hermann, W. *Boll. Soc. Espan. Ceram. Vidrio*: *Proc. XVI Int. Congr. on Glass*, Madrid, 1992, **Vol. 31-C**, P. 233.
61. Donnadieu, P. *J. Non-Cryst. Solids,*1988, **99**, 113.
62. Leko, V. K. *Properties of Silica Glasses*. Institute of Silicate Chemistry, Odoevskogo 24/2, St. Petersburg, Russia.
63. Leko, V. K. & Meshcheryakova, E. V. *Fiz. Khim. Stekla,* 1976, **2**, 317.
64. Leko, V. K. & Meshcheryakova, E. V. *Fiz. Khim. Stekla,* 1976, **2**, 311.
65. Mazurin, O. V., Klyuev, V. P. Leko, V. K. & Meshcheryakova, E. V. *Fiz. Khim. Stekla,* 1975, **1**, 371.
66. Pavlova G. A. & Amatuni, A. N. *Neorg. Mater*., 1975, **11**, 1686.
67. Paek, U. C. Schroeder, C. M. and Kurkjian C. R., *Glass Technology* 1988, **29** (6), 263–6.
68. Hagy, H. E. *J. Am. Ceram. Soc*., 1963, **46**, 93.
69. Scherer, G. W. *Glastech. Ber*., 1983, **56K**, 834.
70. Schultz, P. C. *J. Am. Ceram. Soc*., 1976, **59**, 214.
71. Ohashi, M., Tateda, M., Tajima, K. & Shiraki, K. *Electron. Lett*., 1992, **28**, 1008.
72. Shiraki, K., Ohashi, M., Tajima, K., Tateda, M. & Tsujikawa, K. *Electron. Lett*., 1993, **29**, 1263.
73. Tajima, K., Tateda, M. & Ohashi, M. *J. Lightwave Technol*., 1994, **12**, 411.
74. Mazurin, O. V., Leko, V. K. & Komarova, L. A. *J. Non-Cryst. Solids,* 1975, **18**, 1.
75. Leko, V. K., Meshcheryakova, E. V., Gusakova, N. K. & Lebedeva, R. B. *Opt. Mekh. Prom*., 1974, **12**, 42.
76. Leko, V. K., Meshcheryakova, E. V. & Gusakova, N. K. *Neorg. Mater*., 1975, **11**, 130.
77. Leko, V. K. & Gusakova, N. K. *Fiz. Khim. Stekla,* 1977, **3**, 226.
78. SciGlass 5.0 ™, SciGlass Dictionary (1996–2002) Scivision.
79. Nascimento, M. L. F. & Zanotto, E. D. *Phys. Rev. B,* 2006, **73**, 024209.
80. Jackson, K. A. In *Growth and Perfection of Crystals*. Edited by R. H. Doremus, B. W. Roberts & D. Turnbull, Wiley, New York, 1958.
81. Mai, C., Sekkat, A., Etienne S. & Perez, J. *Proc. Second Int. Conf. Fundamentals in Glass Science and Technology*, 1993, P. 447.
82. Nassau, K., Levy, R. A. & Chadwick, D. L. *J. Electrochem. Soc*., 1985, **132**, 409.
83. Yongman, R. E., Kieffer, J., Bass, J. D. & Dufrene, L. *J. Non-Cryst. Solids,* 1997, **222**, 190.
84. Herron, L. W. & Bergeron C. G. *Phys. Chem. Glasses,* 1978, **19** (4), 89–94.
85. Brebéc, G., Seguin, R., Sella, C., Bevenott, J. & Martin, J. C. *Acta Met*., 1980, **28**, 327.
86. Clark, T. M., Grandinetti, P. J., Florian, P. & Stebbins, J. F. *Phys. Rev. B,* 2004, **70**, 064202
87. Jorgensen, P. J. & Norton, F. J. *Compt. Rend. VII Congr. Intern. du Verre*, Bruxelles, 1965, **Vol. 2**, 1965, P. 310.
88. Kalen, J. D., Boyce, R. S. & Cawley, J. D. *J. Am. Ceram. Soc*., 1991, **74**, 203.
89. Williams, E. L. *J. Am. Ceram. Soc*., 1965, **48**, 190.
90. Muehlenbachs, K. & Schaeffer, H. A. *Canad. Mineral*., 1977, **15**, 179.
91. Haul, R. & Dümbgen, G. *Z. Elektrochem*., 1962, **66**, 636
92. Sucov, E. *J. Am. Ceram. Soc*., 1963, **46**, 14.
93. Yinnon, H. *PhD Thesis,* 1977. Case Western Reserve University.
94. Schaeffer, H. A. *J. Non-Cryst. Solids,* 1980, **38–39**, 545.
95. Kajihara, K. Miura, T. Kamioka, H. Hirano, M. Skuja L. & Hosono, H. *J. Ceram. Soc. Jpn*., 2004, **112**, 559.
96. Norton, F. J. *Nature* 1961, **191**, 701.
97. Hetherington, G. & Jack, K. H. *Phys. Chem. Glasses,* 1964, 5 (5), 147–51.
98. Mikkelsen, J. C. *Appl. Phys. Lett*., 1984, **45**, 1187
99. Cawley, J. D. & Boyce, R. S. *Philos. Mag. A,* 1988, **58**, 589.
100. Ham, C. J. & Helms, C. R. *J. Appl. Phys*., 1986, **59**, 1767.
101. Costello, J. A. & Tressler, R. E. *J. Electrochem. Soc*., 1984, **131**, 1944.
102. Pfeffer R. & Ohring, M. *J. Appl. Phys*., 1981, **52**, 777.
103. Takahashi, T., Fukatsu, S., Itoh, K. M., Uematsu, M., Fujiwara, A., Kageshima, H., Takahashi, Y. & Shiraishi, K. *J. Appl. Phys*. 2003, **93**, 3674.
104. Mathiot, D., Schunk, J. P., Perego, M., Fanciulli, M., Normand, P., Tsamis C. & Tsoukalas, D. *J. Appl. Phys*. 2003, **94**, 2136.
105. Tsoukalas, D., Tsamis C. & Stoemenos, J. *Appl. Phys. Lett*., 1993, **63**, 3167.
106. Tsoukalas, D., Tsamis, C. & Normand, P. *J. Appl. Phys*. 2001, **89**, 7809.